In vivo Zoom Imaging using Transmit SENSE

I. Graesslin[1], S. Boetzl[1], U. Katscher[1], K. Nehrke[1], B. Annighoefer[2], G. Mens[3], and P. Börnert[1]
[1]Philips Research Laboratories, Hamburg, Germany, [2]TU Hamburg-Harburg, Hamburg, Germany, [3]Philips Healthcare, Best, Netherlands

Introduction Zoom imaging allows an increase of the spatial resolution in the targeted region of interest (ROI) without increasing the scan time. Alternatively, maintaining spatial resolution, zoom imaging allows a reduction of the scanning time by reducing the field of view (FOV) to the ROI. For both techniques, potential backfolding artefacts from body regions outside the reduced FOV can be suppressed via local excitation [1]. This local excitation can be performed by multi-dimensional RF pulses, which can be accelerated using spatial transmit sensitivity encoding instead of full gradient encoding [2].
This paper presents (first) zoom imaging volunteer experiments carried out on an 8-transmit channel 3T MRI system [3], with a fully integrated real-time SAR validation prior to the scan allowing the safe use of spatially selective Transmit SENSE RF pulses [4,5] and their fast calculation [6,7,8] for optimal workflow.

Methods The safety concept was implemented on an eight-channel transmit 3T MRI system [3] (based on Achieva, Philips Healthcare, Netherlands). To allow for an efficient workflow for parallel transmit experiments, (A) the SAR calculation as well as (B) Transmit SENSE pulse calculation prior to scanning needs to be sufficiently fast. These two aspects were achieved as described below.
(A) The fast SAR calculation of parallel transmit pulses was realized by pre-calculating the bio-mesh information and storing it in a so-called Q-matrix data base. In this approach, E-fields were determined by FDTD simulation ("XFDTD MicroCluster", Remcom Inc., USA) for multiple dielectric body models according to [9] including the "Visible Human Male" [10]. The calculations for the models were carried out for an ideally decoupled 3T eight-channel body coil [11] for 18 different patient positions in the coil. Then, the pre-calculated E-fields of each element of the TX array were averaged according to [12]. The Q-matrices allow for a sub-millisecond calculation of the local and global SAR on a high-performance graphics card (GeForce GTX280, EVGA® Corporation, USA) with 240 processors. The different models are stored in a Q-matrix data base. For the actual SAR calculation, the fields are superimposed and weighted with the corresponding RF waveforms [13].
(B) The pulse calculation algorithms were parallelized and optimized for fast execution. Three different algorithms were available for calculating the Transmit SENSE RF pulses [2]: an RF power optimized approach [6], a global SAR optimized approach and [7] a global/local SAR optimized approach [10,8]. First, the matrix inversion of the power optimized RF pulse calculation is based on an iterative conjugate gradient method in the image domain. Thus, pulses are calculated within a few seconds for a typical field-of-excitation (FOX) matrix size of 32×32 and a reduction factor of $R \geq 4$. Second, for the global SAR optimized algorithm, the computation time was reduced by parallelization and optimisation to a few seconds on an 8 CPU work station with Intel™ dual QuadCore Xeon E5405@2GHz or a graphics card (see above). Third, a local SAR optimized SOCP algorithm is solving a large-scale constrained optimization problem. This problem can significantly be accelerated by integrating a re-orthogonalized Lanczos algorithm using an iterative decomposition of the matrix to be inverted into a lower rank approximation [10,8].
The work flow is as follows: After the survey scan, the B0 and B1 maps were acquired. In the pulse calculation graphical user interface (GUI), the survey image acts as a background image, and the desired excitation pattern (pixels to be excited in the FOX) can be selected (see Fig. 1, top). First the B0 and B1 maps and the appropriate Q-matrix of the bio-mesh model are selected according to patient-specific information, like body position and sex. This information is used for the SAR optimized RF pulse calculation using the chosen algorithm as described above. Bloch simulations are used to validate the expected excitation pattern, which is displayed in the GUI (see Fig. 1, bottom). The RF pulse is uploaded to the scanner subsequently. The local and global SAR are re-calculated for the current RF pulses and checked for potential violations of given global / local SAR limits.
For the *in vivo* experiments, B1 mapping was performed in healthy volunteers using an inverted AFI (Actual Flip Angle Imaging) technique [14,15] (480×480×60mm³ FOV, 64×64×3 matrix, flip angle = 50°, TR1 = 20ms, TR2 = 100ms, TE=2.3ms, transverse slice orientation), resulting in 22 seconds scan time per 3D B1 map. Spiral k-space trajectories were used with a numerical FOX matrix size of 32×32 and 48×48 pixels and a reduction factor R=4 using the global SAR optimized algorithm. For Transmit SENSE scans, turbo field echo (TFE) was applied with a turbo factor of eight, 480×480 mm² FOX, 480×300 mm² FOV, slice thickness 30mm, TR=40ms, TE=2.3ms, transverse slice orientation. For reception, a 6-channel cardiac SENSE coil was used using a sum-of-squares reconstruction.

Results and Discussion An example for zoom imaging is demonstrated in Figs. 1-5. Figure 1 shows a scout image with the chosen target pattern for local excitation (top) and the forward simulation of the excitation pattern (bottom). The anatomical image corresponding to full FOV and scan time is shown for standard slice selective excitation (Fig. 2) and accelerated local excitation (Fig. 3). Figure 4 shows the zoomed ROI with a 2-fold reduction of the scan time by reducing the field of view (FOV) to the ROI, maintaining spatial resolution. Figure 5 shows the zoomed ROI with spatial resolution increased by a factor of 3 while increasing scan time only by 30%.

Conclusion First *in vivo* results using spatially selective RF pulses for local excitation / zoom imaging were carried out on an 8-channel transmit platform with fully integrated safety mechanisms for the SAR calculation prior to the scan and RF waveform monitoring during the scan. The accelerated calculation of the required RF pulses was integrated on the scanner console with a flexible GUI. A short computation time for the SAR calculation and RF pulse calculations prior to the scan is important for an efficient work flow for in vivo parallel TX experiments. The presented study is regarded as a step towards making zoom imaging feasible in a clinical environment.

Acknowledgements We would like to thank Sven Biederer, Ferdinand Schweser, Hanno Homann, David Brunner, and Klaas Pruessmann for discussions and support.

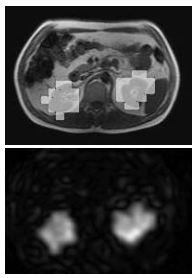

Fig. 1: Scout image with target pattern for the local excitation (top), simulation (bottom).

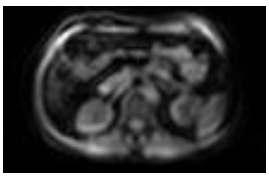

Fig. 2: Image with full FOV 480×300 mm and full scan time, standard slice-selective excitation.
(resolution 7.5×7.5 mm)

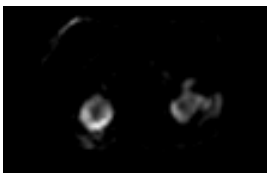

Fig. 3: Image with full FOV 480×300 mm and full scan time, 4× accelerated local excitation.
(resolution 7.5×7.5 mm)

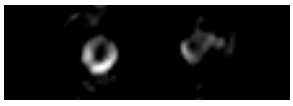

Fig.4: Zoom imaging with a 2-fold reduction of the scan time by reducing the field of view (FOV) to the ROI 480×150 mm, maintaining spatial resolution of 7.5×7.5 mm.

Fig. 5: Zoom imaging with spatial resolution increased by a factor of 3 (2.5×2.5 mm) in the targeted region of interest (ROI) 480×100 mm increasing scan time by only 30%.

References
[1] Ullmann P, et al., [2006] ISMRM 14:598
[2] Katscher U, et al. [2003] MRM 49:144-150
[3] Graesslin I, et al. [2006] ISMRM 14:129
[4] Grissom W, et al. [2006] ISMRM 14:3015
[5] Brunner DO, et al. [2010] MRM 63:1280-1291
[6] Graesslin I, et al. [2006] ISMRM 14:2470
[7] Graesslin I, et al. [2008] ISMRM 16:621
[8] Graesslin I, et al. [2010] ISMRM 18:4932
[9] Homann H, et al. [2010] ISMRM 18:3874
[10] NLM [1996] "Visible Human Project"
[11] Vernickel P, et al. [2007] MRM 58(2):381-9
[12] IEEE Inc. [2002] Std C95, 3rd Ed.
[13] Graesslin I, et al. [2008] ISMRM 16:74
[14] Yarnykh VL MRM [2007] 57(1):192-200
[15] Nehrke K, et al. [2009] MRM 61(1):84-92